Pion and Kaon Distribution Amplitudes from Lattice QCD

Jun Hua,[1,2,3] Min-Huan Chu,[3,4] Fang-Cheng He,[5] Jin-Chen He,[6,7] Xiangdong Ji,[7] Andreas Schäfer,[8] Yushan Su,[7] Peng Sun,[9] Wei Wang,[3] Ji Xu,[3,10] Yi-Bo Yang,[5,11,12,13,*] Fei Yao,[14] Jian-Hui Zhang,[15,14,†] and Qi-An Zhang[16]

(Lattice Parton Collaboration)

[1]*Guangdong Provincial Key Laboratory of Nuclear Science, Institute of Quantum Matter, South China Normal University, Guangzhou 510006, China*
[2]*Guangdong-Hong Kong Joint Laboratory of Quantum Matter, Southern Nuclear Science Computing Center, South China Normal University, Guangzhou 510006, China*
[3]*INPAC, Shanghai Key Laboratory for Particle Physics and Cosmology, Key Laboratory for Particle Astrophysics and Cosmology (MOE), School of Physics and Astronomy, Shanghai Jiao Tong University, Shanghai 200240, China*
[4]*Yang Yuanqing Scientic Computering Center, Tsung-Dao Lee Institute, Shanghai Jiao Tong University, Shanghai 200240, China*
[5]*CAS Key Laboratory of Theoretical Physics, Institute of Theoretical Physics, Chinese Academy of Sciences, Beijing 100190, China*
[6]*School of Physics and Astronomy, Shanghai Jiao Tong University, Shanghai 200240, China*
[7]*Department of Physics, University of Maryland, College Park, Maryland 20742, USA*
[8]*Institut für Theoretische Physik, Universität Regensburg, D-93040 Regensburg, Germany*
[9]*Department of Physics and Institute of Theoretical Physics, Nanjing Normal University, Nanjing, Jiangsu, 210023, China*
[10]*School of Physics and Microelectronics, Zhengzhou University, Zhengzhou, Henan 450001, China*
[11]*School of Fundamental Physics and Mathematical Sciences, Hangzhou Institute for Advanced Study, UCAS, Hangzhou 310024, China*
[12]*International Centre for Theoretical Physics Asia-Pacific, Beijing/Hangzhou, China*
[13]*School of Physical Sciences, University of Chinese Academy of Sciences, Beijing 100049, China*
[14]*Center of Advanced Quantum Studies, Department of Physics, Beijing Normal University, Beijing 100875, China*
[15]*School of Science and Engineering, The Chinese University of Hong Kong, Shenzhen 518172, China*
[16]*School of Physics, Beihang University, Beijing 102206, China*

(Received 28 January 2022; revised 4 September 2022; accepted 8 September 2022; published 23 September 2022)

We present a state-of-the-art lattice QCD calculation of the pion and kaon light-cone distribution amplitudes (DAs) using large-momentum effective theory. The calculation is done at three lattice spacings $a \approx \{0.06, 0.09, 0.12\}$ fm and physical pion and kaon masses, with the meson momenta $P_z = \{1.29, 1.72, 2.15\}$ GeV. The result is nonperturbatively renormalized in a recently proposed hybrid scheme with self-renormalization, and extrapolated reliably to the continuum as well as the infinite momentum limit. We find a significant deviation of the pion and kaon DAs from the asymptotic form, and a large $SU(3)$ flavor breaking effect in the kaon DA.

DOI: 10.1103/PhysRevLett.129.132001

Introduction.—Light pseudoscalar mesons play a fundamental role in quantum chromodynamics (QCD) as they are the (pseudo) Nambu-Goldstone bosons associated with dynamical chiral symmetry breaking [1,2], an important nonperturbative phenomena in the standard model. Their internal structure and its impact on experimental measurements have been actively investigated for many years.

The leading-twist pion and kaon light-cone distribution amplitudes (DAs) are among the simplest physical quantities characterizing such internal structure, and provide a probability amplitude interpretation on how the longitudinal momentum of the pion or kaon is distributed among quarks in its leading Fock state [3]. They are critical inputs for the description of hard exclusive reactions, such as the B meson weak decays [4,5] that provide useful information on CP violation and the Cabibbo-Kobayashi-Maskawa matrix, and play a crucial role for probes of new physics [6]; they are also important for the study of the pion elastic form factors [7], the pion-photon transition form factor [8–10], and of hard exclusive meson production that may give access to nucleon generalized parton distributions [11,12].

Published by the American Physical Society under the terms of the Creative Commons Attribution 4.0 International license. Further distribution of this work must maintain attribution to the author(s) and the published article's title, journal citation, and DOI. Funded by SCOAP³.

At the asymptotically large renormalization scale, it is well-known that these DAs follow a simple form, $\phi(x) = 6x(1-x)$ [3], as other components are suppressed logarithmically through anomalous dimensions of higher-spin operators. However, their shapes at hadronic scales are a nonperturbative QCD problem. A QCD sum rule calculation for the pion DA has stimulated much theoretical debate and many experimental measurements [13–16]. In the past few decades, various nonperturbative models and phenomenological analyses have been proposed to understand this interesting physical quantity; see, for example, Refs. [17–19]. Clearly, a first-principle calculation from lattice QCD will shed more light on this issue.

There have been many lattice studies on the pion and kaon DAs using the traditional moments approach [20–26]. The proposal of large-momentum effective theory (LaMET) [27–29] allows one to access the entire x dependence of the DAs from first-principle lattice calculations, instead of only the first few moments (for other proposals with applications to the DAs, see Refs. [30–33]). Using LaMET, several calculations of the x dependence of meson DAs have been carried out [34–37]. However, a recent analysis [38] showed that the nonperturbative renormalization of the quasi-light-front (quasi-LF) correlation in LaMET could be highly nontrivial, especially when off-shell quark matrix elements are used. In such a case, even after renormalization there may still be residual linear divergences rendering the continuum extrapolation problematic. To resolve this issue, a self-renormalization strategy [39] has been proposed, where one fits the divergence structure to a quasi-LF correlation and uses it for renormalization. The present Letter provides the first full implementation of this strategy, and shows that it indeed gives promising results.

Lattice simulation.—Let us begin with the following definition of the leading-twist light-cone DA of a pseudoscalar meson:

$$\int \frac{d\xi^-}{2\pi} e^{ixp^+\xi^-} \langle 0|\bar{\psi}_1(0) \not{n} \gamma_5 U(0,\xi^-)\psi_2(\xi^-)|M(P)\rangle = i f_M (p\cdot n)\phi_M(x), \tag{1}$$

where $U(0,\xi^-) = P\exp[ig_s\int_{\xi^-}^0 ds\, n\cdot A(sn)]$ is the path-ordered gauge link defined along the minus light-cone direction n ($n^2 = 0$). To extract this quantity, we calculate the following quasi-LF correlation on the lattice with momentum $\vec{P}$ along the z direction [34]:

$$C_2^m(z,\vec{P},t) = \int d^3y e^{-i\vec{P}\cdot\vec{y}} \langle 0|\mathcal{O}_{\Gamma_1}(z;\vec{y},t)\bar{\psi}_2(0,0)\Gamma_2\psi_1(0,0)|0\rangle,$$

where $\mathcal{O}_{\Gamma_1}(z;\vec{y},t) \equiv \bar{\psi}_1(\vec{y},t)\Gamma_1 U(\vec{y},\vec{y}-z\hat{z})\psi_2(\vec{y}-z\hat{z},t)$ is the quasi-LF operator with $\hat{z}$ being the unit vector in the z direction, $U(\vec{x},\vec{x}-\vec{z})$ is the spatial Wilson line connecting lattice sites $\vec{x}$ and $\vec{x}-\vec{z}$, $\psi_2\Gamma_2\psi_1$ is the interpolating field of the meson m, and $\Gamma_{1,2}$ are chosen as $\Gamma_1 = \gamma_z\gamma_5$, $\Gamma_2 = \gamma_5$ for the pseudoscalar meson. The ground-state matrix elements can be extracted from the following two-state fit formula:

$$\frac{C_2^m(z,\vec{P},t)}{C_2^m(z=0,\vec{P},t)} = \frac{H_m^B(z)(1+c_m(z)e^{-\Delta E t})}{(1+c_m(0)e^{-\Delta E t})}, \tag{2}$$

where $H_m^B(z)$ is the normalized ground-state matrix element, c_m and ΔE are free parameters accounting for (one or more) excited state contamination, which are exponentially suppressed in the large time limit. Based on the comparison of one- and two-state fits (see Supplemental Material [40]), we use the one-state fit results in the analysis below with $t_{\rm min} = 0.72$, 0.54, 0.42 fm (for $P_z = 1.29$, 1.72, 2.15 GeV), which is large enough to eliminate the excited states contamination.

TABLE I. Details of the simulation setup. The light and strange quark mass (both valence and sea quark) of the clover action are tuned such that $m_\pi = 140$ MeV and $m_{\eta_s} = 670$ MeV.

Ensemble	a (fm)	$L^3\times T$	$c_{\rm SW}$	$m_{u/d}$	m_s
a06m130	0.057	$96^3\times 192$	1.034 93	−0.0439	−0.0191
a09m130	0.088	$64^3\times 96$	1.042 39	−0.0580	−0.0174
a12m130	0.121	$48^3\times 64$	1.050 88	−0.0785	−0.0191

In this Letter, the simulation is done using the clover fermion action on three ensembles with $2+1+1$ flavors of highly improved staggered quarks generated by the MILC Collaboration [41,42], at physical pion mass with three lattice spacings: 0.057, 0.088, and 0.121 fm. Hypercubic smeared fat links [43] are used in both the fermion action and the quasi-LF operators in C_2^m to improve the signal-to-noise ratio. The rest of the simulation setup is summarized in Table I. In addition, we use momentum smeared $2-2-2$ grid sources, repeat the calculation at several time slices, and average the forward and backward correlation functions to improve statistics. In total, we have 570 (configurations) × 8 (grid source) × 8 (source time slices) × 2 (forward or backward), $730\times 8\times 6\times 2$, and $970\times 8\times 4\times 2$ measurements at three ensembles with $a = 0.057$, 0.088, and 0.121 fm, respectively.

Hybrid scheme with self-renormalization.—The bare quasi-LF correlation calculated above contains both linear and logarithmic ultraviolet (UV) divergences that have to be removed by renormalization. On the lattice, the numerical subtraction of linear divergences is extremely delicate. In particular, such divergences may not be fully removed if the RI/IMOM renormalization scheme is used [38]. We also try the RI/IMOM scheme [44] with different momentum transfer Q^2 at the current operator, and found that the linear divergence can be sensitive to Q^2 in certain cases [40]. Thus, simple modifications on the momentum setup of the RI/IMOM scheme cannot solve the problem.

Here, we adopt the self-renormalization proposed in Ref. [39], which amounts to fitting the bare quasi-LF correlation and subtracting the relevant UV divergences. To be more precise, one fits the bare quasi-LF correlation at given hadron momentum and multiple lattice spacings with a perturbative-QCD-dictated parametrization that contains a linear divergence, a logarithmic divergence, and discretization effects. After removing all the UV divergences and discretization effects, one is left with the renormalized quasi-LF correlation encoding the intrinsic nonperturbative physics.

As suggested in Ref. [39], the UV divergences in the quasi-LF correlator can be determined by using, e.g., the pion parton distribution function (PDF) matrix elements $\mathcal{M}(z) \equiv \langle \pi | \mathcal{O}_{\gamma_t} | \pi \rangle$ in the rest frame at multiple lattice spacings, and fitting the bare data $\mathcal{M}^B$ to the following form [39]:

$$\mathcal{M}^B(z,a) = Z^{\text{self}}(z,a)\mathcal{M}^R(z), \tag{3}$$

with the renormalization factor parametrized as [39]

$$\begin{aligned} Z^{\text{self}}(z,a) \equiv \exp\Bigg\{ & \frac{kz}{a\ln[a\Lambda_{\text{QCD}}]} + m_0 z + f(z)a \\ & + \frac{3C_F}{b_0}\ln\left\{\frac{\ln[1/(a\Lambda_{\text{QCD}})]}{\ln[\mu/\Lambda_{\text{QCD}}]}\right\} \\ & + \ln\left[1 + \frac{d}{\ln(a\Lambda_{\text{QCD}})}\right]\Bigg\}, \end{aligned} \tag{4}$$

where the first term in the curly bracket is the linear divergence, m_0 denotes a finite mass contribution arising from renormalon ambiguity, etc., and $f(z)a$ accounts for the discretization effects. (The $\mathcal{O}(a)$ correction here arises from the mixed action effect in using clover valence fermions on highly improved staggered quark sea ones.) The last two terms come from the resummation of leading and subleading logarithmic divergences, which only affect the overall normalization at different lattice spacings. To partially account for higher-order perturbative effects as well as remaining lattice artifacts, we also treat d and Λ_{QCD} as fitting parameters [39]. The renormalized matrix element is required to be equal to the continuum perturbative $\overline{\text{MS}}$ result at short distances (chosen to be $z \in z_s = [0.06, 0.18]$ fm as defined in [45]),

$$\begin{aligned} \mathcal{M}^R(z)|_{z\in z_s} &= \mathcal{M}^{\overline{\text{MS}},\text{1-loop}}(z) \\ &\equiv 1 + \frac{\alpha_s^{\overline{\text{MS}}} C_F}{4\pi}\left[3\ln\frac{z^2\mu^2}{4e^{-2\gamma_E}} + 5\right] + \mathcal{O}(\alpha_s^{2,\overline{\text{MS}}}), \end{aligned} \tag{5}$$

which helps the determination of m_0 and d. In the calculation we use the $\overline{\text{MS}}$ renormalization scale $\mu = 2$ GeV and $\Lambda_{\overline{\text{MS}}} = 0.24$ GeV.

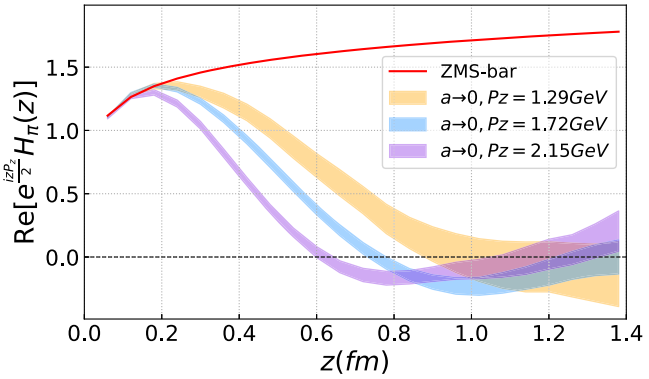

FIG. 1. Comparison of self-renormalized quasi-LF correlation $\text{Re}[e^{(izP_z/2)}H_m^{\overline{\text{MS}}}(z)]$ of the pion with different momenta (bands), and the perturbative result in the $\overline{\text{MS}}$ scheme $H_m^{\overline{\text{MS}},\text{1-loop}}(z)$ (red curve).

In the present case, we follow the same strategy as above, except that the renormalized matrix element in the $\overline{\text{MS}}$ scheme,

$$H_m^{\overline{\text{MS}}}(z) = H_m^B(z,a)/\tilde{Z}^{\text{self}}(z,a), \tag{6}$$

is now required to be matched to the continuum perturbative $\overline{\text{MS}}$ result of the normalized quasi-DA matrix element at short distances in the rest frame, which reads at one loop

$$H_m^{\overline{\text{MS}},\text{1-loop}}(z) \equiv 1 + \frac{\alpha_s^{\overline{\text{MS}}} C_F}{4\pi}\left[3\ln\frac{z^2\mu^2}{4e^{-2\gamma_E}} + 7\right]. \tag{7}$$

$\tilde{Z}^{\text{self}}$ turns out to be the same as Z^{self} except for the value of d.

In Fig. 1, we show a comparison between the self-renormalized quasi-LF correlations $\text{Re}[e^{(izP_z/2)}H_m^{\overline{\text{MS}}}(z)]$ (after linear $\mathcal{O}(a)$ continuum extrapolation and phase rotation) with the perturbative one-loop result $H_m^{\overline{\text{MS}},\text{1-loop}}(z)$. As can be seen from the figure, all quasi-LF correlations agree well with the perturbative result for small z, indicating a mild P_z dependence in that region.

It is worth pointing out that the self-renormalization strategy above does not apply at very small z due to finite lattice spacing artifacts in the data. In the ratio scheme [46], some degree of cancellation happens in the bare correlations between large momentum states and nonperturbative lattice renormalization factors. However, in the present case, the agreement of the self-renormalized LF correlation with the perturbative result extends down to $z \sim 0.06$ fm, which is our smallest lattice spacing. Thus, we only need to supplement it with the renormalized quasi-LF correlation at $z = 0$, which is normalized to 1. In this way, we obtain the fully renormalized quasi-LF correlation. To facilitate the subsequent matching procedure, we define a modified renormalized correlation by further dividing out the

perturbative factor $H_m^{\overline{\rm MS},1\text{-loop}}(z)$ so that the ratio scheme matching applies:

$$H_m^R(z) = \frac{H_m^B(z,a)}{\tilde{Z}^{\rm self}(z,a)\cdot H_m^{\overline{\rm MS},1\text{-loop}}(z)} = \frac{H_m^{\overline{\rm MS}}(z)}{H_m^{\overline{\rm MS},1\text{-loop}}(z)}. \tag{8}$$

Note that this is equivalent to using the hybrid renormalized quasi-LF correlation and matching, as the perturbative difference in the quasi-LF correlation is exactly compensated by that in the matching.

From Fig. 1, we can see that the uncertainty of the renormalized quasi-LF correlation grows rapidly at large distance. A brute-force truncation of the correlation introduces unphysical oscillations [36] in momentum space after Fourier transformation. To resolve this issue, we adopt a physics-based extrapolation form [45] at large quasi-LF distance ($\lambda = zP_z$):

$$H_m^R(z,P_z) = \left[\frac{c_1}{(i\lambda)^a} + e^{-i\lambda}\frac{c_2}{(-i\lambda)^b}\right] e^{-\lambda/\lambda_0}, \tag{9}$$

where the algebraic terms in the square bracket account for a power law behavior of the DAs in the endpoint region and the exponential term comes from the expectation that at finite momentum ($\vec{P}$) the correlation function has a finite correlation length (denoted as λ_0) that becomes infinite when the momentum goes to infinity. In this Letter, the Lorentz boost factor γ for the pion at the physical point is very large $\{9.21, 12.29, 15.36\}$, and thus the correlation length is very large. We therefore drop the $e^{-\lambda/\lambda_0}$ factor, and directly perform a polynomial extrapolation, as suggested in [45]. The details of this extrapolation can be found in the Supplemental Material [40].

Numerical results.—We perform a phase rotation $e^{izP_z/2}$ to the renormalized quasi-LF correlation, so that the imaginary part directly reflects the flavor asymmetry between the strange and up or down quarks. As an example, in Fig. 2, the imaginary part of $e^{izP_z/2}H_m^R(z)$ for the pion (upper panel) and kaon (lower panel) at different lattice spacings with $P_z = 2.15$ GeV. It reflects the SU(3) flavor breaking effects between the valence quarks in the light meson. For the pion it is consistent with zero within errors as expected, since we have used degenerate valence u/d quark masses in the ensembles. While in the case of kaon there is a nonvanishing imaginary part, such an imaginary part increases slightly with P_z, as observed in previous DA studies using LaMET [36,45], and a comparison of the results at different momenta can be found in the Supplemental Material [40].

The factorization can be done either in momentum space [47,48] or in coordinate space. Here, we choose the latter, which results in

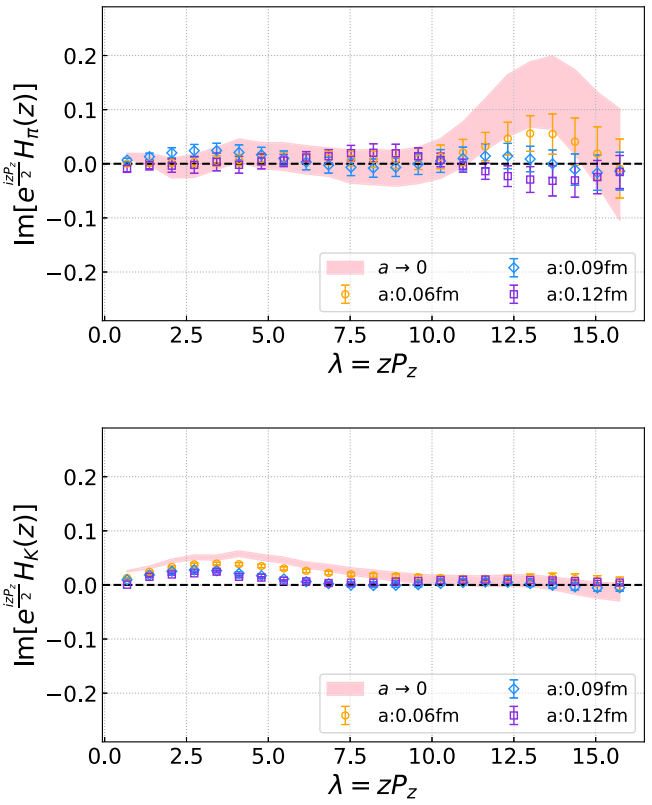

FIG. 2. The imaginary part of the quasi-LF correlation function $[e^{izP_z/2}H_m^R(z)]$ for the pion (top) and kaon (bottom) in the continuum limit $a \to 0$. The hadron momentum is $P_z = 2.15$ GeV.

$$H_m^R(z,\lambda,\mu_R) = \int_0^1 dxdy\,\theta(1-x-y) \times C(x,y,z^2,\mu_R,\mu)h_m^R(x,y,\lambda,\mu) + \mathcal{O}(\Lambda_{\rm QCD}^2 z^2, M^2 z^2), \tag{10}$$

where we take renormalization scale and factorization scale to be the same and set $\mu = \mu_R = 2$ GeV in this Letter. h_m^R is the LF correlation related to the light-cone DA through the following Fourier transformation:

$$h_m^R(x,y,\lambda,\mu) = \int_0^1 du\, e^{iu(x-1)\lambda - i(1-u)y\lambda}\phi(u,\mu). \tag{11}$$

The perturbative matching kernel C up to the next-to-leading order is given in the Supplemental Material [40].

The impact of the perturbative matching is illustrated in Fig. 3, where a Fourier transformation to momentum space has been performed. As can be seen from the figure, the matching broadens the quasi-DA in the physical region. Outside the physical region ($x < 0$ or $x > 1$), there still exists a nonvanishing tail, indicating potential effects of higher-order matching and higher-twist contributions. Nevertheless, in the unphysical region, the results are consistent with zero within ~2 standard deviations.

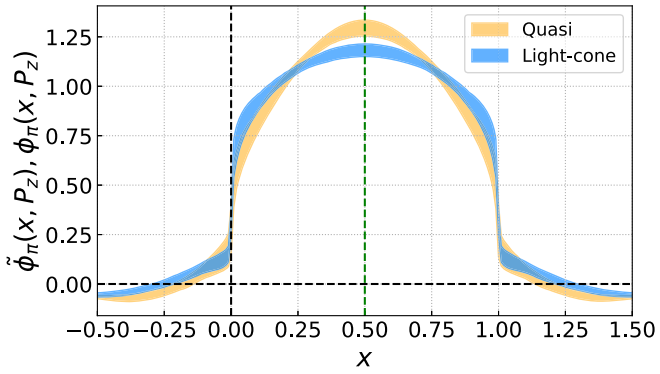

FIG. 3. Quasi-DA and DA for the pion in momentum space in the continuum limit $a \to 0$, $P_z = 2.15$ GeV.

With the results for $P_z = 1.29, 1.72, 2.15$ GeV above, we can perform an extrapolation to $P_z \to \infty$ using the following functional form:

$$\phi(x,P_z) = \phi(x,P_z \to \infty) + \frac{c_2(x)}{P_z^2} + \mathcal{O}\left(\frac{1}{P_z^4}\right). \quad (12)$$

The final results of the π, K DAs are given in Fig. 4, where systematic uncertainties from renormalization scale μ dependence, large λ extrapolation, and continuum and infinite momentum extrapolation have been taken into account. While the systematic uncertainty from continuum extrapolation dominates for the kaon, the statistical (larger than for the kaon due to the lighter quark mass) and continuum extrapolation uncertainties are comparable and dominate for the pion. Therefore, we expect that the kaon DA uncertainty can get significantly suppressed when data at smaller lattice spacings are available that enable us to do a more reliable continuum extrapolation; whereas for the pion, besides data at smaller lattice spacings, we also need increasing statistics to reduce the statistical uncertainty [40]. In the endpoint region, which cannot be reliably predicted by LaMET, we adopt a phenomenological $x^a(1-x)^b$ extrapolation (taken as $0 < x < 0.1$ and $0.9 < x < 1$). The unreliable region is expected to shrink if a larger P_z can be reached in future calculations. For comparison, we also plot the asymptotic form $6x(1-x)$ and results from QCD sum rules [49], Dyson-Schwinger equations (DSE) [50], and reconstructed from moments calculations (OPE) [26]. As can be seen from the figure, both π and K DAs deviate significantly from the asymptotic form, but are close to the results from DSE and OPE calculations. The shape of π DA is much broader than the asymptotic form, manifesting the impact of dynamical chiral symmetry breaking at such a low scale. A similar behavior has also been observed in a recent analysis using QCD sum rules with nonlocal condensates [51].

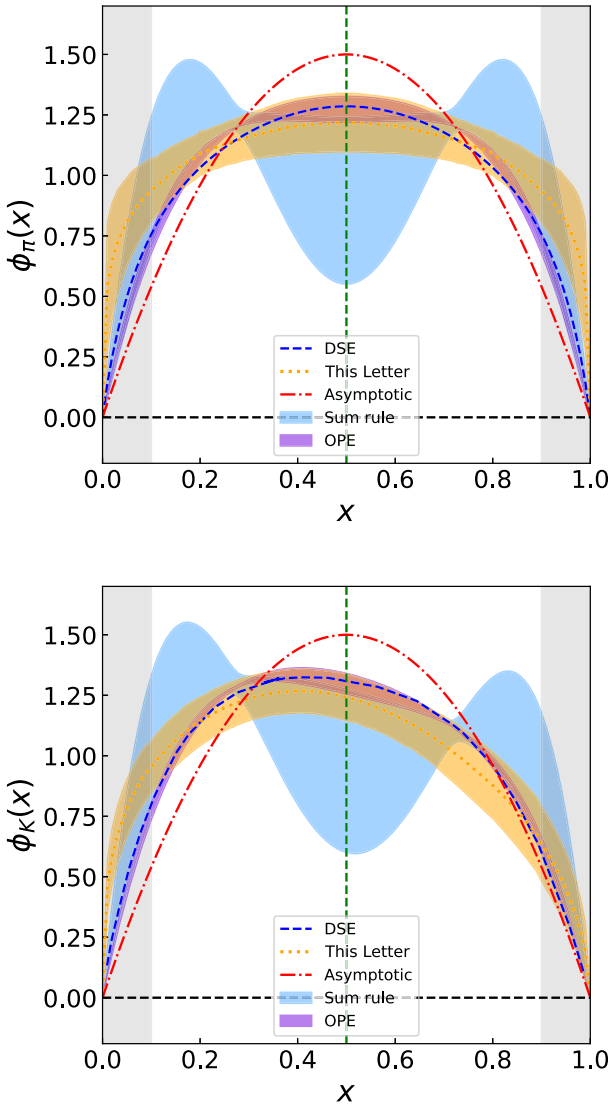

FIG. 4. DAs for π (top) and K (bottom), extrapolated to the continuum ($a \to 0$) and infinite momentum limit ($P_z \to \infty$). For the kaon, x is the momentum fraction carried by the light quark.

Summary.—We present a state-of-the-art lattice calculation of π and K DAs using LaMET. The renormalization is done in the hybrid scheme with self-renormalization proposed recently. Based on the results at physical light and strange quark masses with three lattice spacings and momenta, we perform an extrapolation to the continuum and infinite momentum limit. The final results exhibit a significant deviation from the asymptotic form, while they are close to the DSE and OPE results, especially in the middle x region where our method is reliable. However, there are still some significant differences in the endpoint regions. This could be due to missing higher-power or high-order corrections in LaMET that can be improved in future calculations, or due to effects of higher moments ignored in the OPE and DSE calculations. A more accurate determination of the endpoint behavior of the DAs would

be an important step toward a better understanding of quantities like the pion-photon transition form factor.

The calculations were performed using the Chroma software suite [52] with QUDA [53–55] through HIP programming model [56]. This work is supported in part by the Strategic Priority Research Program of Chinese Academy of Sciences (No. XDB34030302 and No. XDPB15), the National Natural Science Foundation of China (NNSFC) under Grants No. 11735010, No. 11975051, No. 12005130, No. 12047503, No. 11905126, No. U2032102,12125503, a NSFC-DFG joint grant under Grant No. 12061131006 and SCHA 458/22, and Natural Science Foundation of Shanghai under Grant No. 15DZ2272100. X. J. is supported partially by the US DOE, Office of Science, Grant No. DE-SC0020682. The computations were performed on the CAS SunRising-1 computing environment, and also HPC Cluster of ITP-CAS. Part of the numerical computations has been tested on the cluster at National Supercomputing center in Zhengzhou, and Siyuan-1 cluster supported by the Center for High Performance Computing at Shanghai Jiao Tong University.

*Corresponding author.
ybyang@mail.itp.ac.cn
†Corresponding author.
zhangjianhui@cuhk.edu.cn

[1] S. Weinberg, Physica (Amsterdam) **96A**, 327 (1979).
[2] S. Weinberg, *The Quantum Theory of Fields. Vol. 2: Modern Applications* (Cambridge University Press, Cambridge, England, 2013).
[3] G. P. Lepage and S. J. Brodsky, Phys. Lett. **87B**, 359 (1979).
[4] H.-Y. Cheng and C.-K. Chua, Phys. Rev. D **80**, 114008 (2009).
[5] F. Su, Y.-L. Wu, Y.-B. Yang, and C. Zhuang, J. Phys. G **38**, 015006 (2011).
[6] R. Aaij *et al.* (LHCb Collaboration), Phys. Rev. Lett. **122**, 191801 (2019).
[7] G. R. Farrar and D. R. Jackson, Phys. Rev. Lett. **43**, 246 (1979).
[8] Y.-M. Wang and Y.-L. Shen, J. High Energy Phys. 12 (2017) 037.
[9] V. M. Braun, A. N. Manashov, S. Moch, and J. Schonleber, Phys. Rev. D **104**, 094007 (2021).
[10] J. Gao, T. Huber, Y. Ji, and Y.-M. Wang, Phys. Rev. Lett. **128**, 062003 (2022).
[11] X.-D. Ji, Phys. Rev. Lett. **78**, 610 (1997).
[12] A. V. Radyushkin, Phys. Lett. B **385**, 333 (1996).
[13] V. L. Chernyak and A. R. Zhitnitsky, Nucl. Phys. **B201**, 492 (1982); **B214**, 547(E) (1983).
[14] J. Gronberg *et al.* (CLEO Collaboration), Phys. Rev. D **57**, 33 (1998).
[15] B. Aubert *et al.* (*BABAR* Collaboration), Phys. Rev. D **80**, 052002 (2009).
[16] S. Uehara *et al.* (Belle Collaboration), Phys. Rev. D **86**, 092007 (2012).
[17] E. R. Arriola and W. Broniowski, Phys. Rev. D **66**, 094016 (2002).
[18] L. Chang, I. C. Cloet, J. J. Cobos-Martinez, C. D. Roberts, S. M. Schmidt, and P. C. Tandy, Phys. Rev. Lett. **110**, 132001 (2013).
[19] N. G. Stefanis, Phys. Rev. D **102**, 034022 (2020).
[20] M. Goeckeler, R. Horsley, D. Pleiter, P. E. L. Rakow, A. Schaefer, G. Schierholz, W. Schroers, and J. M. Zanotti, Nucl. Phys. B, Proc. Suppl. **161**, 69 (2006).
[21] V. M. Braun, M. Göckeler, R. Horsley, H. Perlt, D. Pleiter, P. E. L. Rakow, G. Schierholz, A. Schiller, W. Schroers, H. Stüben, and J. M. Zanotti, Phys. Rev. D **74**, 074501 (2006).
[22] P. A. Boyle, M. A. Donnellan, J. M. Flynn, A. Juttner, J. Noaki, C. T. Sachrajda, and R. J. Tweedie (UKQCD Collaboration), Phys. Lett. B **641**, 67 (2006).
[23] R. Arthur, P. A. Boyle, D. Brommel, M. A. Donnellan, J. M. Flynn, A. Juttner, T. D. Rae, and C. T. C. Sachrajda, Phys. Rev. D **83**, 074505 (2011).
[24] V. M. Braun, S. Collins, M. Göckeler, P. Pérez-Rubio, A. Schäfer, R. W. Schiel, and A. Sternbeck, Phys. Rev. D **92**, 014504 (2015).
[25] G. S. Bali, V. M. Braun, M. Göckeler, M. Gruber, F. Hutzler, P. Korcyl, B. Lang, and A. Schäfer (RQCD Collaboration), Phys. Lett. B **774**, 91 (2017).
[26] G. S. Bali, V. M. Braun, S. Bürger, M. Göckeler, M. Gruber, F. Hutzler, P. Korcyl, A. Schäfer, A. Sternbeck, and P. Wein (RQCD Collaboration), J. High Energy Phys. 08 (2019) 065; 11 (2020) 37.
[27] X. Ji, Phys. Rev. Lett. **110**, 262002 (2013).
[28] X. Ji, Sci. China Phys. Mech. Astron. **57**, 1407 (2014).
[29] X. Ji, Y. Liu, Y.-S. Liu, J.-H. Zhang, and Y. Zhao, Rev. Mod. Phys. **93**, 035005 (2021).
[30] V. Braun and D. Müller, Eur. Phys. J. C **55**, 349 (2008).
[31] G. S. Bali, V. M. Braun, B. Gläßle, M. Göckeler, M. Gruber, F. Hutzler, P. Korcyl, B. Lang, A. Schäfer, P. Wein, and J.-H. Zhang, Eur. Phys. J. C **78**, 217 (2018).
[32] G. S. Bali, V. M. Braun, B. Gläßle, M. Göckeler, M. Gruber, F. Hutzler, P. Korcyl, A. Schäfer, P. Wein, and J.-H. Zhang, Phys. Rev. D **98**, 094507 (2018).
[33] W. Detmold, A. Grebe, I. Kanamori, C. J. D. Lin, S. Mondal, R. Perry, and Y. Zhao, Phys. Rev. D **105**, 034506 (2022).
[34] J.-H. Zhang, J.-W. Chen, X. Ji, L. Jin, and H.-W. Lin, Phys. Rev. D **95**, 094514 (2017).
[35] J.-H. Zhang, L. Jin, H.-W. Lin, A. Schäfer, P. Sun, Y.-B. Yang, R. Zhang, Y. Zhao, and J.-W. Chen (LP3 Collaboration), Nucl. Phys. **B939**, 429 (2019).
[36] R. Zhang, C. Honkala, H.-W. Lin, and J.-W. Chen, Phys. Rev. D **102**, 094519 (2020).
[37] J. Hua, M.-H. Chu, P. Sun, W. Wang, J. Xu, Y.-B. Yang, J.-H. Zhang, and Q.-A. Zhang (Lattice Parton Collaboration), Phys. Rev. Lett. **127**, 062002 (2021).
[38] K. Zhang, Y.-Y. Li, Y.-K. Huo, A. Schäfer, P. Sun, and Y.-B. Yang (χQCD Collaboration), Phys. Rev. D **104**, 074501 (2021).
[39] Y.-K. Huo *et al.* (Lattice Parton Collaboration (LPC) Collaboration), Nucl. Phys. **B969**, 115443 (2021).
[40] See Supplemental Material at http://link.aps.org/supplemental/10.1103/PhysRevLett.129.132001 for more details of the analysis.

[41] E. Follana, Q. Mason, C. Davies, K. Hornbostel, G. P. Lepage, J. Shigemitsu, H. Trottier, and K. Wong (HPQCD and UKQCD Collaborations), Phys. Rev. D **75**, 054502 (2007).
[42] A. Bazavov *et al.* (MILC Collaboration), Phys. Rev. D **87**, 054505 (2013).
[43] A. Hasenfratz and F. Knechtli, Phys. Rev. D **64**, 034504 (2001).
[44] C. Sturm, Y. Aoki, N. H. Christ, T. Izubuchi, C. T. C. Sachrajda, and A. Soni, Phys. Rev. D **80**, 014501 (2009).
[45] X. Ji, Y. Liu, A. Schäfer, W. Wang, Y.-B. Yang, J.-H. Zhang, and Y. Zhao, Nucl. Phys. **B964**, 115311 (2021).
[46] K. Orginos, A. Radyushkin, J. Karpie, and S. Zafeiropoulos, Phys. Rev. D **96**, 094503 (2017).
[47] X. Ji, A. Schäfer, X. Xiong, and J.-H. Zhang, Phys. Rev. D **92**, 014039 (2015).
[48] Y.-S. Liu, W. Wang, J. Xu, Q.-A. Zhang, S. Zhao, and Y. Zhao, Phys. Rev. D **99**, 094036 (2019).
[49] P. Ball, V. M. Braun, and A. Lenz, J. High Energy Phys. 08 (2007) 090.
[50] C. D. Roberts, D. G. Richards, T. Horn, and L. Chang, Prog. Part. Nucl. Phys. **120**, 103883 (2021).
[51] N. G. Stefanis, Phys. Lett. B **738**, 483 (2014).
[52] R. G. Edwards and B. Joo (SciDAC, LHPC, and UKQCD Collaborations), Nucl. Phys. B, Proc. Suppl. **140**, 832 (2005).
[53] M. A. Clark, R. Babich, K. Barros, R. C. Brower, and C. Rebbi, Comput. Phys. Commun. **181**, 1517 (2010).
[54] R. Babich, M. A. Clark, B. Joo, G. Shi, R. C. Brower, and S. Gottlieb, in *Proceedings of the SC11 International Conference for High Performance Computing, Networking, Storage and Analysis Seattle, Washington, 2011* (Association for Computing Machinery, New York, 2011), arXiv:1109.2935.
[55] M. A. Clark, B. Jo, A. Strelchenko, M. Cheng, A. Gambhir, and R. Brower, arXiv:1612.07873.
[56] Y.-J. Bi, Y. Xiao, M. Gong, W.-Y. Guo, P. Sun, S. Xu, and Y.-B. Yang, Proc. Sci. LATTICE2019 (**2020**) 286.